KineticTheoretic Description of Shock Wave Formation. II.

C. K. Chu

Citation: Physics of Fluids (1958-1988) **8**, 1450 (1965); doi: 10.1063/1.1761439
View online: http://dx.doi.org/10.1063/1.1761439
View Table of Contents: http://scitation.aip.org/content/aip/journal/pof1/8/8?ver=pdfcov
Published by the AIP Publishing

Kinetic-Theoretic Description of Shock Wave Formation. II.

C. K. Chu
Columbia University, New York, New York
(Received 16 February 1965)

The method and results previously obtained [C. K. Chu, Phys. Fluids 8, 12 (1965)] for a one-dimensional gas ($\gamma = 3$) is extended to a monatomic three-dimensional gas ($\gamma = 5/3$). The classical Riemann problem—the flow of a gas in a shock tube—is treated as an initial value problem for the Krook equation, after the Krook equation is first reduced to two simultaneous Krook equations each for a one-dimensional gas. The numerical scheme used is the same as that previously proposed. Results are obtained on the formation of shocks corresponding to Mach numbers of 1.27, 1.5, and 1.75. It is seen that the stronger the shock, the shorter the formation time. The short-time behavior of the flow agrees with free flow, while the long-time behavior agrees with fluid dynamics. The shocks formed agree very closely with the results of Liepmann, Narasimha, and Chahine.

INTRODUCTION

In a previous paper,[1] we investigated by numerical computation the formation of a shock wave in a shock tube for a "one-dimensional" gas (a gas with one degree of freedom in thermal motion) as an initial value problem of the Krook equation. We pointed out that while the one-dimensional gas is not a physically realistic model, it does give us much qualitative insight and numerical experience; and at the end of Ref. 1, we gave a procedure by means of which the Krook equation for a regular gas (three-dimensional gas) can be reduced to two simultaneous Krook equations, each for a one-dimensional gas. This permits us to carry out computations on a three-dimensional gas without requiring unmanageable computing capacities. The present paper gives the results of these computations.

There are some interesting and important physical consequences that were not interpretated in Ref. 1, since it was felt that the gas was too hypothetical to put much faith in. These phenomena again appear in this paper, and we analyze them in greater detail. Specifically missing in Ref. 1 is any indication of the relation between the strength of a shock and its formation time; questions of this nature will be studied in this paper.

In the first section, we concisely summarize the theoretical development and numerical procedure, as already presented in detail in Ref. 1. This permits the present paper to be logically self-contained, although for motivations, philosophical discussions, etc., the reader should see Ref. 1. In the next section, computed results are presented and interpretations given. The final section contains suggestions for extensions and future research based on the experience gathered in these two papers.

[1] C. K. Chu, Phys. Fluids 8, 12 (1965).

SUMMARY OF MATHEMATICAL FORMULATION AND NUMERICAL PROCEDURE

The initial value problem for the Krook equation in one space dimension consists of the equation:

$$\frac{\partial f}{\partial t} + \xi \frac{\partial f}{\partial x} = \kappa \frac{n}{n^*}(F - f), \tag{1}$$

where

$$n = \iiint_{-\infty}^{\infty} f \, d\xi \, d\eta \, d\zeta, \qquad nu = \iiint_{-\infty}^{\infty} \xi f \, d\xi \, d\eta \, d\zeta,$$

$$\tfrac{3}{2}nR\theta = \iiint_{-\infty}^{\infty} \tfrac{1}{2}[(\xi - u)^2 + \eta^2 + \zeta^2] f \, d\zeta \, d\eta \, d\zeta, \tag{2}$$

and

$$F = \frac{n}{(2\pi R\theta)^{\frac{3}{2}}} \exp\left[-\frac{(\xi - u)^2 + \eta^2 + \zeta^2}{2R\theta}\right], \tag{3}$$

subject to the initial conditions

$$f(x, \xi, t) = \phi(x, \xi) \quad \text{at} \quad t = 0. \tag{4}$$

Here t is the time, x the space coordinate, $\xi = (\xi, \eta, \zeta)$ the particle velocity, n, u, θ the density, macroscopic velocity (in x direction) and temperature, respectively, n^* some reference density, R the gas constant for the particular gas (given by Boltzmann constant/molecular mass), $f = f(x, \xi, t)$ the distribution function, and $F = F(x, \xi, t)$ the local Maxwellian distribution function. The collision frequency κ is taken as constant for simplicity except when noted, but may just as well be chosen to fit the viscosity law desired.

As it stands, f is a function of five arguments, which renders numerical computations virtually impossible on present day computers because of the excessive storage capacity required. For one-di-

mensional problems, however, it is possible to reduce the problem (1) to (4) to an initial value problem for two simultaneous Krook equations, each governing a function of only three independent variables and coupled through the macroscopic quantities. (Independently, this reduction also appears in Ref. 2.) We define

$$g(x, \xi, t) = \int_{-\infty}^{\infty}\int_{-\infty}^{\infty} f(x, \xi, t)\, d\eta\, d\zeta, \tag{5}$$

$$h(x, \xi, t) = \int_{-\infty}^{\infty}\int_{-\infty}^{\infty} (\eta^2 + \zeta^2) f(x, \xi, t)\, d\eta\, d\zeta. \tag{6}$$

Then, integrating out the η and ζ dependence in (1) to (4), we get the equivalent system

$$\begin{aligned} \frac{\partial g}{\partial t} + \xi \frac{\partial g}{\partial x} &= \kappa \frac{n}{n^*}(G - g), \\ \frac{\partial h}{\partial t} + \xi \frac{\partial h}{\partial x} &= \kappa \frac{n}{n^*}(H - h), \end{aligned} \tag{7}$$

where

$$\begin{aligned} n &= \int_{-\infty}^{\infty} g\, d\xi, \qquad nu = \int_{-\infty}^{\infty} \xi g\, d\xi, \\ \tfrac{3}{2} nR\theta &= \int_{-\infty}^{\infty} \tfrac{1}{2}(\xi - u)^2 g\, d\xi + \tfrac{1}{2}\int_{-\infty}^{\infty} h\, d\xi, \end{aligned} \tag{8}$$

and

$$\begin{aligned} G &= \iint_{-\infty}^{\infty} F\, d\eta\, d\zeta = \frac{n}{(2\pi R\theta)^{\frac{1}{2}}} \exp\left[-\frac{(\xi - u)^2}{2R\theta}\right], \\ H &= \iint_{-\infty}^{\infty} (\eta^2 + \zeta^2) F\, d\eta\, d\zeta \\ &= n\left(\frac{2R\theta}{\pi}\right)^{\frac{1}{2}} \exp\left[-\frac{(\xi - u)^2}{2R\theta}\right], \end{aligned} \tag{9}$$

with the initial conditions

$t = 0$:

$$\begin{aligned} g &= \Phi(x, \xi) = \iint_{-\infty}^{\infty} \phi(x, \xi)\, d\eta\, d\zeta, \\ h &= \Psi(x, \xi) = \iint_{-\infty}^{\infty} (\eta^2 + \zeta^2)\phi(x, \xi)\, d\eta\, d\zeta. \end{aligned} \tag{10}$$

For the shock tube problem, the initial data (10) consist of two Maxwellian distributions, one for $x < 0$ and the other for $x > 0$, for two different densities ($n = n_3$ for $x < 0$ and $n = n_0$ for $x > 0$), the same velocity $u = 0$, and the same temperature θ_0.

To describe the finite difference procedure, we first pick the finite difference time step T, such that $\epsilon = \kappa T \ll 1$. We nondimensionalize time t with respect to T, all velocities (macroscopic and microscopic) with respect to $\xi_0 = (2R\theta_0)^{\frac{1}{2}}$, x with respect to $\xi_0 T$, density with respect to n_0 (n^* is also chosen to be n_0), temperature with respect to θ_0, and distribution functions g and h with respect to n_0/ξ_0 and $n_0\xi_0$. The nondimensionalized variables will be denoted by a caret. In terms of them, Eqs. (7)–(10) become

$$\frac{\partial \hat{g}}{\partial \hat{t}} + \hat{\xi}\frac{\partial \hat{g}}{\partial \hat{x}} = \epsilon\hat{n}(\hat{G} - \hat{g}), \quad \frac{\partial \hat{h}}{\partial \hat{t}} + \hat{\xi}\frac{\partial \hat{h}}{\partial \hat{x}} = \epsilon\hat{n}(\hat{H} - \hat{h}); \tag{11}$$

$$\begin{aligned} \hat{n} &= \int_{-\infty}^{\infty} \hat{g}\, d\hat{\xi}, \qquad \hat{n}\hat{u} = \int_{-\infty}^{\infty} \hat{\xi}\hat{g}\, d\hat{\xi}, \\ \hat{n}\hat{\theta} &= \frac{2}{3}\left[\int_{-\infty}^{\infty} (\hat{\xi} - \hat{u})^2 \hat{g}\, d\hat{\xi} + \int_{-\infty}^{\infty} \hat{h}\, d\hat{\xi}\right]; \end{aligned} \tag{12}$$

and

$$\hat{G} = \frac{\hat{n}}{(\hat{\theta}\pi)^{\frac{1}{2}}} \exp\left[-\frac{(\hat{\xi} - \hat{u})^2}{\hat{\theta}}\right], \qquad \hat{H} = \hat{\theta}\hat{G}, \tag{13}$$

with initial conditions

$$\hat{t} = 0: \quad \hat{g} = \hat{\Phi}(\hat{x}, \hat{\xi}), \qquad \hat{h} = \hat{\Psi}(\hat{x}, \hat{\xi}). \tag{14}$$

Within the time step $0 \le t \le T$, i.e., $0 \le \hat{t} \le 1$, we expand $\hat{g}$, $\hat{h}$, $\hat{n}$, $\hat{u}$, $\hat{\theta}$, $\hat{G}$, $\hat{H}$, and $\hat{\Phi}$ and $\hat{\Psi}$ all as power series in ϵ and substitute them into (11)–(14). The zeroth order term, corresponding to the zeroth power of ϵ, gives free flow:

$$\frac{\partial \hat{g}^{(0)}}{\partial \hat{t}} + \hat{\xi}\frac{\partial \hat{g}^{(0)}}{\partial \hat{x}} = 0, \qquad \frac{\partial \hat{h}^{(0)}}{\partial \hat{x}} + \hat{\xi}\frac{\partial \hat{h}^{(0)}}{\partial \hat{x}} = 0,$$

or

$$\begin{aligned} \hat{g}^{(0)}(\hat{x}, \hat{\xi}, \hat{t}) &= \hat{\Phi}(\hat{x}, \hat{\xi}), \\ \hat{h}^{(0)}(\hat{x}, \hat{\xi}, \hat{t}) &= \hat{\Psi}(\hat{x}, \hat{\xi}), \end{aligned} \qquad 0 \le \hat{t} \le 1. \tag{15}$$

The first order term gives the first correction due to collisions:

$$\frac{\partial \hat{g}^{(1)}}{\partial \hat{t}} + \hat{\xi}\frac{\partial \hat{g}^{(1)}}{\partial \hat{x}} = \hat{n}^{(0)}(\hat{G}^{(0)} - \hat{g}^{(0)}),$$

$$\frac{\partial \hat{h}^{(1)}}{\partial \hat{t}} + \hat{\xi}\frac{\partial \hat{h}^{(1)}}{\partial \hat{x}} = \hat{n}^{(0)}(\hat{H}^{(0)} - \hat{h}^{(0)}),$$

[2] G. Bienkowski, paper presented to Fourth International Symposium on Rarefied Gas Dynamics at Toronto (1964).

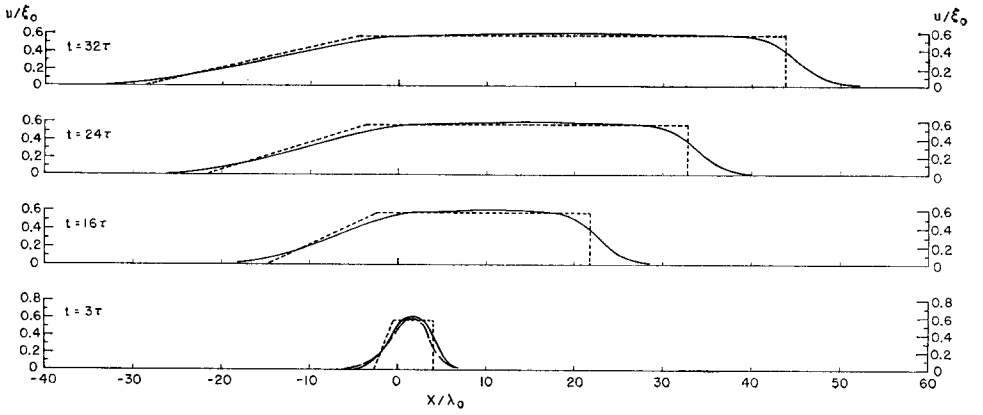

FIG. 1. Velocity distribution in shock tube flow (pressure ratio 8.237:1; shock Mach number 1.5). —— computed results; - - - classical Riemann solution; – – – free-molecular flow.

or

$$\hat{g}^{(1)}(\hat{x}, \hat{\xi}, 1) = \int_0^1 \hat{n}^{(0)}(\hat{x} - \hat{\xi}(1 - \hat{t})) \cdot[\hat{G}^{(0)}(\hat{x} - \hat{\xi}(1 - \hat{t}), \hat{\xi}, \hat{t}) - \hat{g}^{(0)}(\hat{x} - \hat{\xi}(1 - \hat{t}), \hat{\xi}, \hat{t})]\, d\hat{t},$$

$$\hat{h}^{(1)}(\hat{x}, \hat{\xi}, 1) = \int_0^1 \hat{n}^{(0)}(\hat{x} - \hat{\xi}(1 - \hat{t})) \cdot[\hat{H}^{(0)}(\hat{x} - \hat{\xi}(1 - \hat{t}), \hat{\xi}, \hat{t}) - \hat{h}^{(0)}(\hat{x} - \hat{\xi}(1 - \hat{t}), \hat{\xi}, \hat{t})]\, d\hat{t}. \quad (16)$$

The last step is a quadrature, everything on the right-hand side to be integrated being known. The quantities $\hat{n}^{(0)}$, $\hat{u}^{(0)}$, and $\hat{\theta}^{(0)}$ are the corresponding moments of $\hat{g}^{(0)}$ and $\hat{h}^{(0)}$, and $\hat{G}^{(0)}$ and $\hat{H}^{(0)}$ are Maxwell distributions corresponding to the macroscopic variables.

This constitutes our finite difference scheme. Given $\hat{g}$ and $\hat{h}$ at $t = 0$, we calculate these functions and their moments at $t = T$ (i.e., $\hat{t} = 1$) by taking these two terms of the asymptotic expansion. Using the calculated results at $t = T$ as data, we then calculate the functions at $t = 2T$, and so on.

RESULTS AND INTERPRETATIONS

In this section we present and interpret the results of the computations. We first discuss in some detail the shock tube flow for a shock Mach number of 1.5. Those aspects which have already been discussed in Ref. 1 and which are not qualitatively different here, however, are touched upon only lightly. We compare the shock developed with a stationary shock computed by our method, and also compare it with the shock obtained by Liepmann *et al.*[3] We also compare the flow at small time with the results of Bienkowski.[2] Finally, we conclude by comparing the shock formation times for several different shock strengths.

As in Ref. 1, quite apart from how we picked the scaling in the computational procedure, we shall in presenting the results always use the following quantities for uniformity: the unit of time shall be the mean collision time of the low pressure gas ($\tau = 1/\kappa$), the unit of velocity shall be the mean thermal speed at the initial temperature [$\xi_0 = (2R\theta_0)^{\frac{1}{2}}$], the unit of length shall be the mean free path defined as $\lambda_0 = \xi_0\tau$, and the unit of temperature shall be the initial temperature θ_0.

Shock Tube Flow

Calculations for the flow in the shock tube were made at several different pressure ratios. Typical results, valid for a shock Mach number $M = 1.5$ or a driving pressure ratio of 8.237:1, are given in Figs. 1 and 2. Figure 1 gives the distribution of the macroscopic velocity at four time instants: $t = 3\tau$, 16τ, 24τ, and 32τ; Fig. 2 gives the temperature distribution at the same time instants. These calculations were made with mesh sizes $\Delta x = 0.4\xi_0\tau$ and $\Delta\xi = 0.4\xi_0$, $-4.0\xi_0 \leq \xi \leq 4.8\xi_0$. The time step T was chosen such that $\epsilon = T/\tau = 0.1$. The integration (16) was carried out without further subdivision of the time interval, i.e., as a single strip trapezoid. (In the notation of Ref. 1, $m = 1$.) The total time required on the IBM 7094 machine was 37 minutes. This was actually shorter than the time required for the one-dimensional gas problem in Ref. 1 because of a more efficient program. The same parameters were used for the problem with shock Mach number 1.27; but for the problem with shock Mach number 1.75, it was necessary to reduce the time interval to $\epsilon = T/\tau = 0.05$ to avert numerical instability.

[3] H. W. Liepmann, R. Narasimha, and M. T. Chahine, Phys. Fluids 5, 1313 (1962).

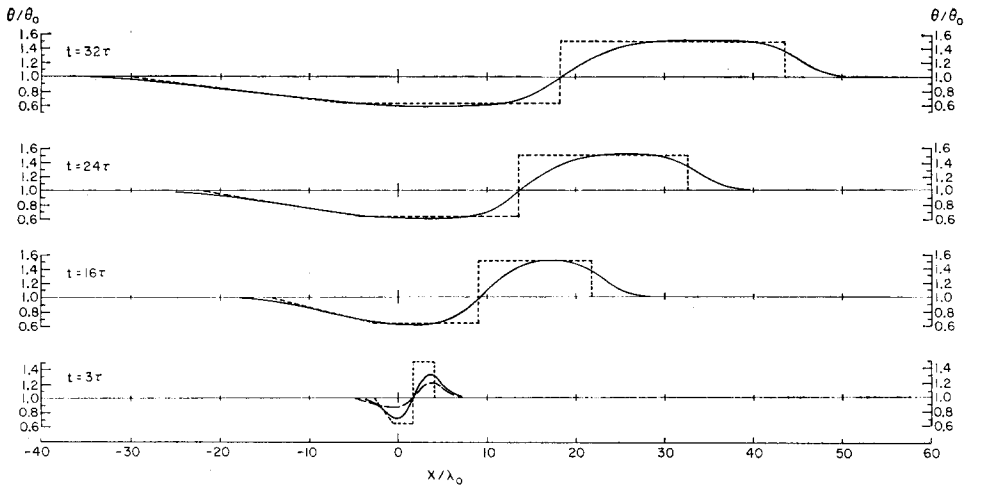

FIG. 2. Temperature distribution in shock tube flow (pressure ratio 8.237:1; shock Mach number 1.5). - - - computed results; —— classical Riemann solution; – – – free-molecular flow.

As in Ref. 1, the computed solution is in very close agreement with the classical results. The rarefraction wave and the uniform regions are closely approximated, the contact discontinuity is replaced by a region whose thickness expands as $t^{\frac{1}{2}}$, and the shock assumes a steady structure after some collisions. At small time, the computed results closely approximate free flow, as is also expected.

One interesting feature that was incorrectly interpreted in Ref. 1 is the "hump" in the velocity distribution in the uniform region. In a one-dimensional gas, the free flow maximum velocity is significantly higher than the continuum value, and it travels at roughly the same speed as the continuum gas velocity. This "hump" was interpreted in Ref. 1 as the remainder of the free-flow peak. In the present case, the "hump" still occurs, and in fact, it is higher than the free-flow peak; moreover, it does not travel at the same velocity as the free-flow peak, but at the same speed as the contact discontinuity (in this case, these two velocities are quite different). The correct explanation is that this is a small diffusion across the contact discontinuity. Since there is a temperature difference but no pressure difference across the contact layer, the hot gas would cool down and thus become denser while the cold gas would become hotter and less dense. This density change is accompanied by a macroscopic flow across the contact layer, which exhibits itself as this "hump."

It is interesting to compare our results at small time with those of Bienkowski.[2] Bienkowski uses a power series expansion for small time and uses the linearized Navier–Stokes equations for large time. Thus, only the small time results are comparable to ours; his large time results are qualitative only. Our results are essentially in good agreement with Bienkowski's. However, since he only goes up to 3 high-pressure collision times (corresponding to 0.9τ for $M = 1.27$ and even smaller for higher Mach numbers), exact agreement is impossible because the finite difference results exhibit strong "graininess" at small times. Thus, his results are more accurate than ours for very small times, when the flow departs only very slightly from free flow, while our results are valid for all subsequent longer times.

Stationary Shock

Again as in Ref. 1, we use our numerical procedure to compute the structure of a stationary shock. This permits us to have a reference, to which we may compare the shock developed in the shock tube; moreover, in the present case, it gives us a comparison with the results of Liepmann *et al.*[3] Since their method is tailored to steady profiles, its accuracy is high; a direct comparison with their results would give us further confidence on the accuracy of our numerical procedure.

The initial data for this calculation consists of two Maxwellian distributions, one on each side of a discontinuity, satisfying the Rankine–Hugoniot conservation conditions. We again note that in the Riemann problem, the conservation laws were never used; the solution to the Krook equation satisfies the conservation equations automatically. Since the conservation equations are used in this stationary shock computation, we would expect the profile to be more accurate.

Figures 3 and 4 show (in solid lines) the velocity and temperature distributions thus computed. As

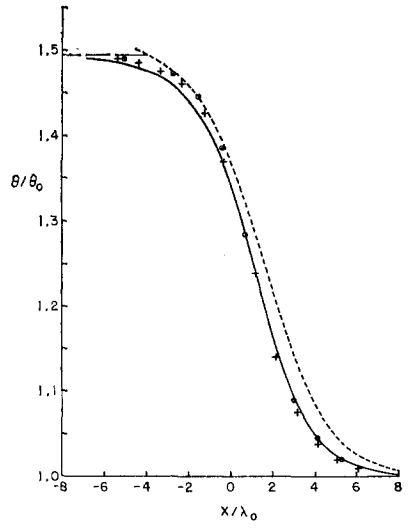

FIG. 3. stationary and well-developed temperature profiles for a 1.5 Mach number shock. —— stationary shock (after 44 collision times); - - - shock developed in shock-tube flow (after 32 collision times); ⊙ results of Liepman *et al.*, and Navier–Stokes solution; + stationary shock computed with $\kappa\alpha\theta^{0.26}$.

in Ref. 1, these profiles are computed accurately in that changing parameters and increasing time steps do not produce further noticeable changes in the results. Also superimposed (in dotted lines) in the same figures are the profiles obtained from the Riemann problem. Again as mentioned in Ref. 1, while the agreement between the stationary shock and the developed shock is acceptably close, a discrepancy does exist. We feel this is due to the fact that while the exact solutions would be identical, a numerical solution of each problem is only an approximation, and this is the inherent discrepancy which presumably would vanish as the mesh size approaches zero.

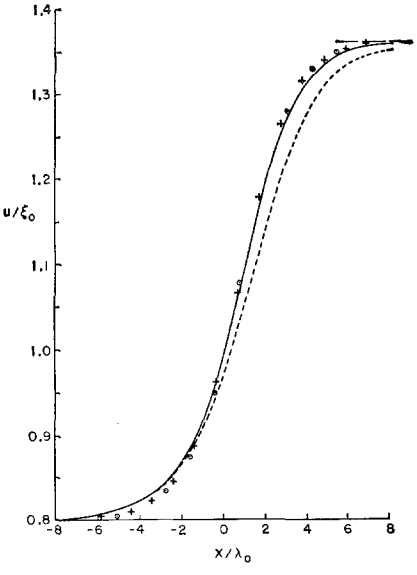

FIG. 4. Stationary and well-developed velocity (relative to shock) profiles for a 1.5 Mach number shock. —— stationary shock (after 44 collision times); - - - shock developed in shock-tube flow (after 32 collision times); ⊙ results of Liepmann *et al.*, and Navier–Stokes solution; + stationary shock computed with $\alpha\theta^{0.26}$.

We note that the origin corresponding to our stationary shock is chosen to be the position of the initial discontinuity and that in the Riemann problem is the location of the discontinuity in the fluid dynamical solution. If we adopt the more conventional usage of defining the origin the point of maximum slope in the velocity profile, then the position of the shock is about one mean free path ahead of the fluid dynamical position at all times.

Also superimposed on these two figures are the results of Liepmann, Narasimha, and Chahine,[3] shown in circles, which at $M = 1.5$ are also just Navier–Stokes results. Their results as given in Ref. 3 have the length scale in terms of Maxwellian mean free paths, which can be related to the Krook time constant throught the viscosity. It is readily seen that the Maxwellian mean free path is related to our $\lambda_0 = \xi_0\tau$ thus:

$$\lambda_0/\lambda_{\text{Maxwell}} = 5\pi^{\frac{1}{2}}/8 = 1.109.$$

This uses the viscosity–Krook constant relation as given in Ref. 2, and also the Maxwellian free path–viscosity relation for hard spheres, which is standard (see, e.g., Jeans[4]). In addition, the origin in Ref. 3 was taken as the point of maximum slope; this is accounted for in the superimposing of the points.

The slight departure of the results of Ref. 3 from ours is due to the fact that while we used a constant κ (corresponding to Maxwellian molecules), Liepmann *et al.* used a Sutherland viscosity law fitted to argon. We recomputed our stationary shock using the same viscosity law; this amounted to adding to κ a dependence on $\theta^{0.26}$. The results are shown as crosses, and the agreement with Liepmann's is indeed most gratifying. This lends strong support to the accuracy of our numerical method.

Formation Time For Shocks of Different Strengths

Figure 5 shows three different sets of profiles at various times, corresponding to shock Mach numbers of 1.27, 1.5, and 1.75. To render a fair comparison, we normalize the temperature rise as is also done by Liepmann *et al.*[3]

$$\Delta\theta_{\text{normal}} = (\theta - \theta_0)/(\theta_1 - \theta_0),$$

[4] J. Jeans, *Kinetic Theory of Gases* (Cambridge University Press, London, 1960).

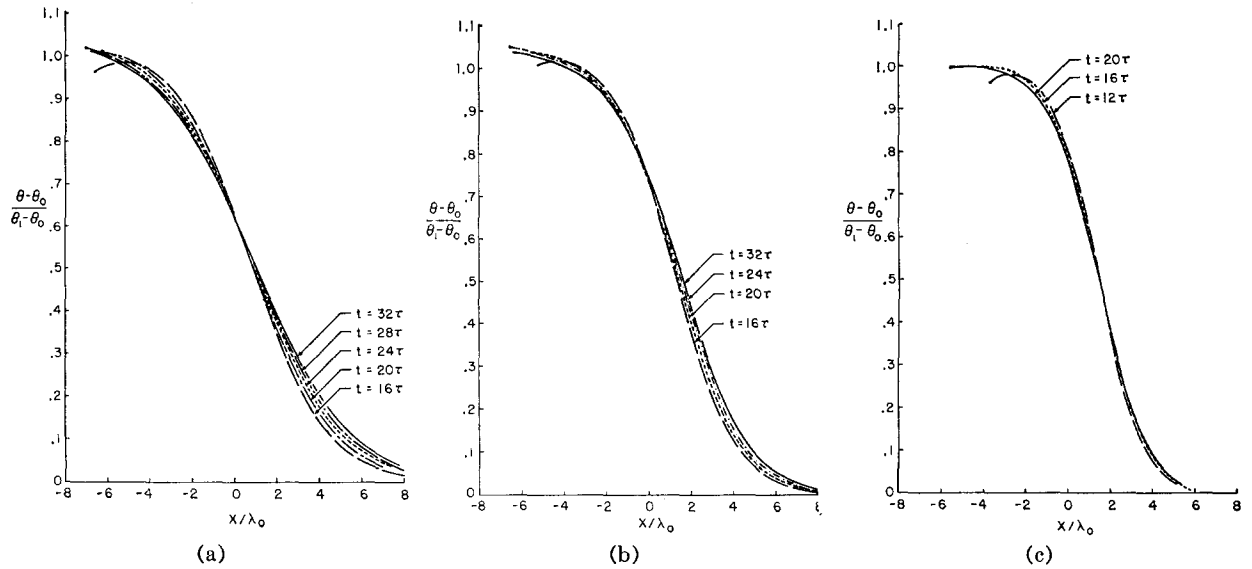

FIG. 5. Normalized temperature profiles showing different formation times for shocks of different strengths in shock-tube flows. (a) Pressure ratio = 3.358, shock Mach number = 1.27. (b) Pressure ratio = 8.237, shock Mach number = 1.50. (c) Pressure ratio = 20.49, shock Mach number = 1.75.

where θ_0 is just 1 and θ_1 is the gas dynamic value, equal to 1.263, 1.495, 1.77 for the three shocks, respectively. It is quite clear that the $M = 1.75$ shock has reached a steady profile after some 16 collision times, the $M = 1.5$ shock reaches a steady profile after some 24 collision times, while the $M = 1.27$ shock is still not quite steady even after 32 collision times; thus, the *stronger the shock, the faster it forms.*

Unfortunately, the present calculation procedure is not yet suitable for strong shocks. It would be interesting to see how this phenomenon continues at higher Mach numbers.

CONCLUDING REMARKS

The present paper together with Ref. 1 completes a preliminary effort to treat numerically unsteady fluid dynamic problems from the viewpoint of kinetic theory. Based on the experience gained, we conclude by indicating some directions in which the present type of study may be extended:

(1) Strong shocks. The present study covers only the formation of relatively weak shocks, with Mach number up to about 2. There is no difficulty in principle in applying the same procedure to stronger shocks, except for the fact that the time step must be shortened, the velocity range must be expanded, and the number of points in the x axis must be increased. This is due to the fact that macroscopic velocities are higher, the shock moves faster and the mean collision time of the high-pressure side gas is smaller. It so happens that on the present IBM 7094 machine, using the present program, $M = 2$ is not far from the upper limit of practicability without the use of tapes for storage. Application to stronger shocks is possible either on large storage machines, or perhaps by a more ingenuous computer program.

(2) Unsteady boundary-value problems. The present study treats pure initial value problems. It would be fruitful to extend the same procedure to unsteady boundary value problems, an immediately obvious example being, say, the piston problem.

(3) Numerical analysis. In the present paper, the finite difference procedure has been used in an experimental spirit. We only know that the procedure is correct when the results are reasonable in comparison with classical results; moreover, we can produce numerical instability simply by increasing ϵ, so that the numerical analysis aspect of the problem is by no means trivial. It would be of interest to be able to answer these questions on a more definitive basis. This would be beneficial for future numerical studies on the Boltzmann equation proper.

ACKNOWLEDGMENTS

The author acknowledges with pleasure the many helpful discussions with Harold Grad, R. A. Gross, and many of the staff members at the Columbia University Plasma Research Laboratory.

This research was sponsored by the Air Force Office of Scientific Research under contract No. AF 49(638)-1254.